Characterization of Porous Low-k Dielectric Thin Films Using X-ray Reflectivity, Small Angle Neutron Scattering and Ion Scattering

Hae-Jeong Lee[1], Eric K. Lin[1], Howard Wang[1], Wen-li Wu[1], Wei Chen[2], and Thomas A. Deis[2]

[1]*National Institute of Standards and Technology, Polymers Division, Gaithersburg, MD, 20899, USA*
[2]*Semiconductor Fabrication Materials KCI, Dow Corning, USA*

Abstract

A novel methodology using a combination of high energy ion scattering, x-ray reflectivity, and small angle neutron scattering is used to characterize the structure and properties of porous low-k dielectric films after varying process conditions. From these techniques we determine the film thickness, average electron density, and density depth profile, wall density, porosity, average pore size, and pore connectivity. When the dielectric constant increases from 1.5 to 2.2, the relative wall density increases by approximately 25 % and relative decreases in the volume fraction of porosity and the average pore size are approximately 10 % and 50 %, respectively.

Introduction

As minimum device dimensions are reduced below 0.18 μm, the increase in propagation delay, cross-talk noise, and power dissipation of the interconnect structure become limiting factors for integrated circuits. To address these problems, new low dielectric constant (low-k) interlayer dielectric materials are being developed to replace the traditional silica. Because it is difficult to reduce the dielectric constant below 2.5 with a fully dense material, it may be necessary to introduce micro- or mesoporosity to achieve very low-k values. The introduction of voids (k =1) decreases the dielectric constant by lowering the average density. If one can vary the porosity in a controlled manner, it should be possible to control the dielectric constant. Unlike traditional nonporous dielectric materials, the detailed structure of the porous network affects other properties crucial to the integrated chip. Therefore it is critical to have methods to characterize the on-wafer structure of these porous thin films to understand and interpret correlations between processing conditions and the resulting physical properties. Currently, there are few experimental techniques able to characterize the porosity of thin films as prepared on a silicon substrate (1-3).

In this work, we provide unique on-wafer measurements of structural properties of hydrogen silsesquioxane (HSQ) based porous thin films (Dow Corning XLK) prepared with a wide range of processing conditions. The methodology employs a combination of small angle neutron scattering (SANS), high-resolution specular x-ray reflectivity (SXR), and ion scattering techniques. We illustrate our methodology and present critical structural information such as the average pore size, pore connectivity, porosity, electron density profile, film thickness, matrix material density, and film elemental composition.

Experimental

Thin films were processed as detailed in a previous article (4). The dielectric constants of these films ranged from 1.5 to 2.2 and the Si-H bond fraction ranged from 30 % to 52 %. The elemental composition of the films was determined using Rutherford backscattering spectrometry (RBS) for silicon, carbon, and oxygen and Forward recoil spectrometry (FRES) for hydrogen. SXR experiments were performed at grazing incident angles on a modified $\theta-2\theta$ x-ray diffractometer at specular conditions with the incident angle equal to the detector angle. The x-ray source is a fine focus copper K_α radiation with a wavelength, λ, of 1.54 Å. Reflectivity fringes due to the constructive and destructive interference from the film surface and the substrate surface were observed. SANS measurements were performed on the 8 m NG1 beam line at the Center for Neutron Research of the National Institute of Standards and Technology. The neutron wavelength was 6 Å with a wavelength spread (FWHM) $\Delta\lambda/\lambda$ of 0.14. The sample to detector distance was 3.6 m and the detector was offset by 3.5° from the incident beam to increase the range of observable angles. Two-dimensional scattering patterns were collected and corrected for empty beam and background scattering using standard reduction methods (3).

Results and Discussion

Fig. 1 shows SXR experimental data and the best fit to the data from a film with a dielectric constant of 2.0 and a Si-H fraction of 35 %. The SXR profile of the film is plotted as the logarithm of the reflected intensity (I_r/I_0) as a function of q ($q = (4\pi/\lambda)\sin\theta$), where, θ is the grazing incident angle of the x-ray beam. At low q values, the reflectivity is unity and the x-ray beam is totally reflected from the sample surface. The reflectivity drops sharply as the x-ray beam begins to penetrate the film after a critical value of q. This critical angle in units of q_c^2 (Å^{-2}) is proportional to the average electron density of the film. Given the elemental composition of the film, this electron density is easily converted into an average mass density. The elemental composition data are summarized in Table 1. The electron density from the critical angle of the film in

Fig. 1 is calculated to be (0.266 ± 0.005) electrons/Å^3 with a resulting average mass density of (0.87 ± 0.01) g/cm^3 (5). The average mass density of the film is also related to the porosity and matrix density of the film through the rule of mixtures, $\rho_{ave} = \rho_w$ (1-P), where, ρ_w is the density of the matrix or wall material and P is the porosity of the film. A second critical angle occurs at slightly higher q values when the x-rays begin to penetrate the silicon substrate. In addition to average mass density, the overall thickness of the film can be determined from the periodicity of the interference fringes through the relationship, thickness = 2π/fringe spacing. The thickness of the film in Fig.1 is calculated to be (7780 ± 10) Å.

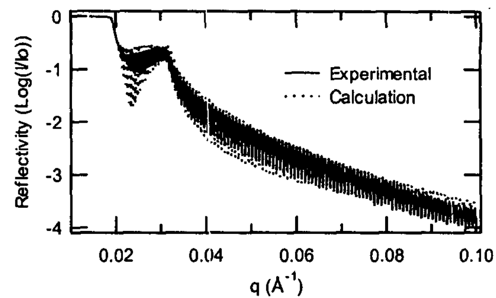

Fig. 1 SXR curve of the film with dielectric constant of 2.0 and Si-H fraction of 35 %. The data are presented the logarithm of the reflected intensity as a function of q. The solid and dotted curves indicate the experimental and calculated dada, respectively.

Table 1. Structural properties of Dow Corning XLK porous thin film varying process condition

Sample	Dielectric Constant	Si-H Fraction (%)	Atomic Composition (Si: O: C: H, %)	Film Thickness (Å)	q_c^2 (E-4) (Å^{-2})	Average Density (g/cm^3)	Pore Size (Å)	Wall Density (g/cm^3)	Porosity (%)
K15_42	1.5	42	27: 49: 8: 16	13290	2.75	0.64	40	1.57	60
K15_49	1.5	49	28: 49: 8: 15	13270	2.71	0.63	41	1.65	62
K20_30	2.0	30	26: 51: 8: 15	10200	3.85	0.89	30	2.10	57
K20_35	2.0	35	25: 49: 9: 17	7780	3.77	0.87	30	2.02	57
K20_47	2.0	47	24: 45: 11: 20	10630	3.52	0.81	27	1.80	55
K20_52	2.0	52	26: 49: 6: 19	7940	3.58	0.83	26	1.98	58
K22_51	2.2	51	26: 50: 8: 16	7570	4.52	1.05	21	2.17	52

The relative standard uncertainties of the atomic composition, film thickness, q_c^2, average density, pore size, wall density, and porosity are ± 5 %, 10 Å, 0.05 Å^{-2}, 0.05 g/cm^3, 1 Å, 0.05 g/cm^3 and 5 %, respectively.

The SXR data are fitted by comparing model electron density profiles to the experimental data using a least squares fitting routine based on the algorithm of Parrat (6). Model profiles with variable thickness and electron density and roughness are adjusted until the calculated reflectivity agrees with the data. Fig. 1 demonstrates the excellent agreement that is obtained between the calculated and experimental data. In Fig. 2, the corresponding electron density depth profile for the SXR data of Fig. 1 shows very uniform electron density profile with a thin densified layer (approximately 230 Å) at the free surface of the film. The SXR measurements for all of the remaining films are shown in Fig. 3 and Fig. 4. As we expected, the first critical angle shifts to lower q values as the dielectric constant decreases, indicating that films with lower k have a lower average density. This trend is quantified in Table 1. Fig. 4 and Table 1 also demonstrate that changes of the Si-H fraction do not significantly change the average density of the films.

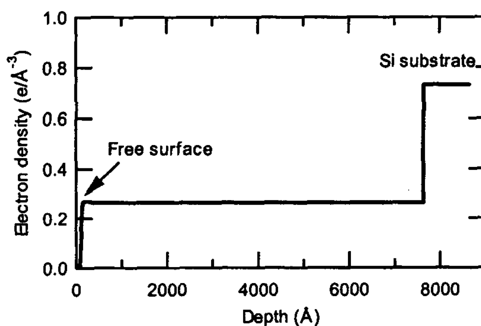

Fig. 2 Calculated electron density profile of the film with dielectric constant of 2.0 and Si-H fraction of 35 %. The free surface is located at the far left of the horizontal axis and the silicon substrate is located at the far right of the abscissa.

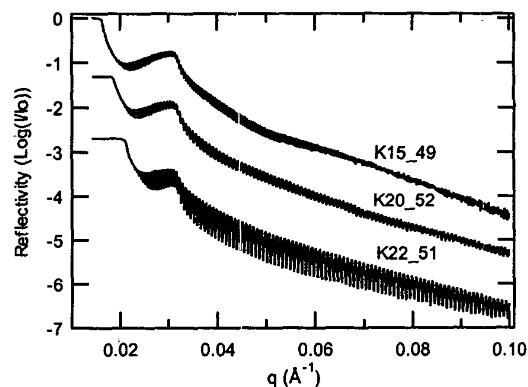

Fig. 3 SXR curves of the HSQ based porous thin films with different dielectric constants.

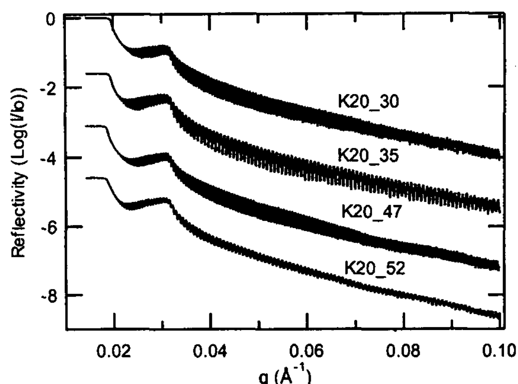

Fig. 4 SXR curves of the HSQ based porous thin films with different Si-H fractions.

The small angle scattering data can be analyzed using the Debye model (7). In this case, the density of the wall material between the pores is assumed to be uniform and the density correlation function describing the structure is assumed to be exponential by $\gamma(r) = \exp(-r/\xi)$, where ξ is the correlation length. Fig. 5 shows the SANS data for both the film in air and immersed in deuterated toluene on an absolute intensity scale as a function of q, where $q = (4\pi/\lambda)\sin(\theta/2)$ and θ is the scattering angle. From the Debye model fits to the data, the average pore size is characterized in terms of the correlation length. Given I(0), which is the scattered intensity at q = 0, and ξ, the equation describing the SANS intensity becomes a function of only ρ_w and P. Similarly, the SXR and RBS measurements provide a relationship between ρ_w and P, which can be used to calculate the average wall density and porosity. The detailed equations are shown in elsewhere (3). Also, the average chord length (average pore size) is given by the equation $l_c = \xi/(1-P)$. For a film with a dielectric constant of 2.0 and a Si-H fraction of 35 %, the porosity was determined to be (0.57 ± 0.05) and the matrix wall density was (2.02 ± 0.05) g/cm^3. Given the porosity, the average pore size is (30 ± 1) Å.

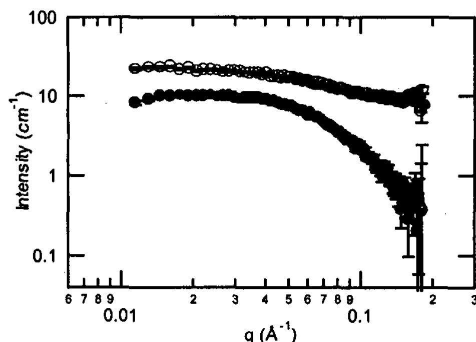

Fig. 5 SANS data of the film with dielectric constant of 2.0 and Si-H fraction of 35 % under ambient conditions (filled symbols) and immersed in deuterated toluene (open symbols).

As shown in Fig. 5, the scattering intensity is significantly stronger for the film immersed in d-toluene than for that in air. The increase in the intensity is due to the enhanced scattering contrast from a deuterated solvent that has penetrated the film. The fraction of pores that are connected and accessible to the film surface can be estimated from the magnitude of the increase in scattering intensity. For this film, the pores were fully connected. Other films after varying processing conditions were characterized in the same way and the results are summarized in Table 1. When the dielectric constant increases from 1.5 to 2.2, the relative wall density increases by approximately 25 % and relative decreases in the volume fraction of porosity and the average pore size are approximately 10 % and 50 %, respectively. Figure 6 shows a linear relationship between dielectric constant and porosity. The data for pure HSQ with dielectric constant of 3.0 is also shown in the figure for comparison (8).

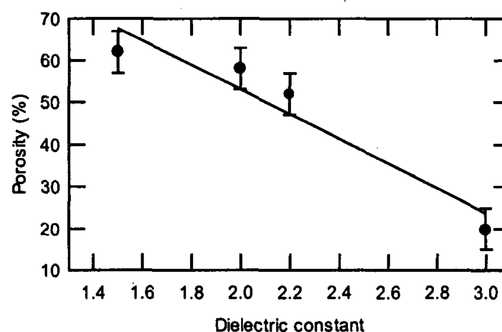

Fig. 6 Relationship between dielectric constant vs porosity

Conclusion

We have applied a non-destructive methodology utilizing information from high energy ion scattering, SXR, and SANS to measure several important structural and physical properties of HSQ based porous thin films with different processing condition. Combining the information from three techniques, we determine the film thickness, electron density depth profile, average film density, matrix material density, porosity, average pore size and pore connectivity.

References

(1) D. W. Gidley, W. E. Frieze, T. L. Dull, A. F. Yee, C. V. Nguyen, and D. Y. Yoon, *Appl. Phys. Lett.*, **76**, 1282 (2000).
(2) F. N. Dultsev, and M. H. Baklanov, *Elect. Solid State Lett.*, **2**, 192 (1999).
(3) W. L. Wu, W. E. Wallace, E. K. Lin, G. W. Lynn, C. J. Glinka, E. T. Ryan, and H. M. Ho, *J. Appl. Phys.* **87**, 1193 (2000).
(4) C. Jin, and J. Wetzel, International Interconnect Technology Conference (IITC) Proceedings, 99, 2000.
(5) The data throughout the manuscript and in the figures are presented along with the standard uncertainty (±) involved in the measurement.
(6) J. Lekner, *Theory of Reflection* (Nijhoff, Dordrecht, 1987).
(7) P. Debye, H. R. Anderson, and H. Brumberger, *J. Appl. Phys.*, **28**, 679 (1957).
(8) H. C. Liou, and J. Pretzer, *Thin solid films*, **335**, 186 (1998).